2019-novel Coronavirus severe adult respiratory distress syndrome in two cases in Italy: An uncommon radiological presentation

Fabrizio Albarello[a], Elisa Pianura[a], Federica Di Stefano[a], Massimo Cristofaro[a], Ada Petrone[a], Luisa Marchioni[a], Claudia Palazzolo[a], Vincenzo Schininà[a,*], Emanuele Nicastri[a], Nicola Petrosillo[a], Paolo Campioni[a], Petersen Eskild[b,c,d], Alimuddin Zumla[e], Giuseppe Ippolito[a], COVID 19 INMI Study Group[1]

[a] Lazzaro Spallanzani, National Institute for Infectious Diseases – IRCCS, Via Portuense, 292, cap 00148 Rome, Italy
[b] Directorate General for Disease Surveillance and Control, Ministry of Health, Muscat, Oman
[c] Institute for Clinical Medicine, Faculty of Health Science, University of Aarhus, Denmark
[d] ESCMID Emerging Infections Task Force, Basel, Switzerland
[e] Department of Infection, Division of Infection and Immunity, University College London, and NIHR Biomedical Research Centre, University College London Hospitals NHS Foundation Trust, London, United Kingdom

A B S T R A C T

Introduction: Several recent case reports have described common early chest imaging findings of lung pathology caused by 2019 novel Coronavirus (SARS-COV2) which appear to be similar to those seen previously in SARS-CoV and MERS-CoV infected patients.
Objective: We present some remarkable imaging findings of the first two patients identified in Italy with COVID-19 infection travelling from Wuhan, China. The follow-up with chest X-Rays and CT scans was also included, showing a progressive adult respiratory distress syndrome (ARDS).
Results: Moderate to severe progression of the lung infiltrates, with increasing percentage of high-density infiltrates sustained by a bilateral and multi-segmental extension of lung opacities, were seen. During the follow-up, apart from pleural effusions, a tubular and enlarged appearance of pulmonary vessels with a sudden caliber reduction was seen, mainly found in the dichotomic tracts, where the center of a new insurgent pulmonary lesion was seen. It could be an early alert radiological sign to predict initial lung deterioration. Another uncommon element was the presence of mediastinal lymphadenopathy with short-axis oval nodes.
Conclusions: Although only two patients have been studied, these findings are consistent with the radiological pattern described in literature. Finally, the pulmonary vessels enlargement in areas where new lung infiltrates develop in the follow-up CT scan, could describe an early predictor radiological sign of lung impairment.

© 2020 The Authors. Published by Elsevier Ltd on behalf of International Society for Infectious Diseases. This is an open access article under the CC BY-NC-ND license (http://creativecommons.org/licenses/by-nc-nd/4.0/).

Introduction

On December 31, 2019, aggregate cases of an apparently new respiratory syndrome were reported in the city of Wuhan, China by Chinese national health authorities to the World Health Organization (WHO) (Huang et al., 2020; Organization WH, 2020a). As of 13h February 2020, there have been 45 171 cases reported to the World

Health Organization with 1104 deaths (Organization WH, 2020a). Outside China there have been 441 confirmed cases reported from 24 countries (Organization WH, 2020a; Organization WH, 2020b). The first two cases detected in Italy were on January 29, 2020, when a couple from the city of Wuhan who travelled to Italy were admitted to the Lazzaro Spallanzani National Institute of Infectious Diseases, in Rome, after becoming ill, presenting with respiratory tract

---

symptoms and fever. Laboratory on respiratory samples tests confirmed infection with SARS-COV2 infection.

Several recent case reports (Chan et al., 2020; Chen et al., 2020; Chung et al., 2020; Kanne, 2020; Koo et al., 2018; Lei et al., 2020; Liu and Tan, 2020; Pan and Guan, 2020; Song et al., 2020; Wang et al., 2020) have described common early chest imaging findings of lung pathology caused by SARS-COV2. These changes appear to be similar to those seen previously in patients with SARS (Ooi et al., 2004; Nestor et al., 2004; Nicolaou et al., 2003) and MERS (Das et al., 2015a; Das et al., 2015b).

The Hubei health commission has express its intention to change the case definition for including "clinically diagnosed cases," in addition to those confirmed by a test, stating that CT scan results will be considered a diagnostic tool for confirmation of suspected cases (Organization WH, 2020c).

We present imaging findings of our two cases of laboratory confirmed COVID-19 in Italy, who progressed to develop adult respiratory distress syndrome (ARDS).

Patient details and clinical presentation

A female and male couple in their 60 s both residents of the city of Wuhan, China, travelled to Italy for holidays. The 66-year-old female patient was under oral hypertension treatment, and the 67-year-old male patient was apparently healthy. On January 28, whilst in Rome, they simultaneously fell ill with respiratory symptoms and fever and were admitted the following day, on January 29, to the high level isolation unit at the Lazzaro Spallanzani National Institute of Infectious Diseases, in Rome, Italy. nasopharyngeal and oropharyngeal swabs from both patients were positive for SARS-COV2 infection when tested using the SARS-COV2 Real-Time Reverse Transcriptase (RT)-PCR (Corman et al., 2020). Both patients developed progressive respiratory failure on day 4 and clinical evidence of ARDS with mechanical ventilation support in intensive care unit was reported on day 6 in the male patient, and, after 12 h on day 7, in the female patient. At the time of submission on February 9 (day 12 since symptom onset), both patients are still mechanically ventilated in Intensive Care Unit in critical but stable clinical conditions.

Imaging studies: chest X-Ray and CT imaging

Chest X-Ray with conventional plain films by using anteroposterior projection at bedside were performed. Baseline volumetric CT scan in the supine position at full inspiration was performed on day 2. Follow-up CT scans on both patients were done on days 3 and 5 to assess for progressive lung impairment. All baseline and follow-up CT scans were performed on a multi-detector row helical CT system scanner (Bright Speed, General Electric Medical

Systems, Milwaukee, WI) using 120 kV pp, 250 mA, pitch of 1.375, gantry rotation time of 0,6 s and time of scan 13 s. The non-contrast scans were reconstructed with slice thicknesses of 0.625 mm and spacing of 0.625 mm with high-resolution lung algorithm. The images obtained on lung (window width, 1,000–1,500 H; level, −700 H) and mediastinal (window width, 350 H; level, 35–40 H) settings were reviewed on a picture archiving and communication system workstation (Impax ver. 6.6.0.145, AGFA Gevaert SpA, Mortsel, Belgium).

Two experienced radiologists in thorax imaging reviewed the radiographs and all CT scans obtained and reached a consensus on findings. The radiographs and CT scans were assessed for the presence and distribution of abnormalities.

Chest X-ray evaluation included: (A) presence of interstitial involvement (reticular, nodular o mixed pattern), (B) presence of lung opacities, (C) presence of pleural effusion, (D) presence of pleural calcification, (E) hilar enlargement, (F) mediastinal lines, (G) cardiac silhouette.

CT scan evaluation included: (Huang et al., 2020) Ground-glass opacities and consolidation (GGO): 1.1 absence of both ground-glass opacities and consolidation; 1.2 presence of pure ground-glass; 1.3 presence of ground glass opacities; 1.4 presence of consolidation; 1.5 presence of ground-glass opacities with consolidation; 1.6 crazy paving. Data (Huang et al., 2020) were assessed for any segment of the five lung lobes. (Organization WH, 2020a) Pleura: 2.1 presence of focal thickening; 2.2 pleural effusion (presence and thickness); 2.3 presence of calcifications. (Organization WH, 2020b) Mediastinum: 3.1 presence of lymphadenopathy (defined as lymph node size of ≥10 mm in short-axis dimension); 3.2 presence of pericardial effusion; 3.3 ascending thoracic aorta diameter. (Chan et al., 2020) Pulmonary vessels: 4.1 perilesional vessels diameter; 4.2 pulmonary artery trunk diameter. Other lung findings (e.g. cavitation, calcification, and bronchiectasis) were noted. Follow-up lung CT were acquired in both patients and these scans were also evaluated to assess the residual pulmonary volume in a preliminary quantitative setting using a thoracic Volume Computer Assisted Reading imaging software (VCAR, GE Medical Systems, Milwaukee, Wis) (Figure 1a, **b, c**).

Imaging findings

In the male patient, a chest X-Ray was performed two days after symptom onset and the chest X-Ray was not consistent with lung alterations. However, one day later, the chest CT scan showed ground-glass opacities and crazy paving (Figures 2a, 3 **a**) in the right upper lobe, in the lateral segment of the middle lobe, and in the superior and posterior-basal segments of the right lower lobe. On the left side, the lesions involved the superior and posterior-basal segments of the lower lobe. Moreover, we found there was
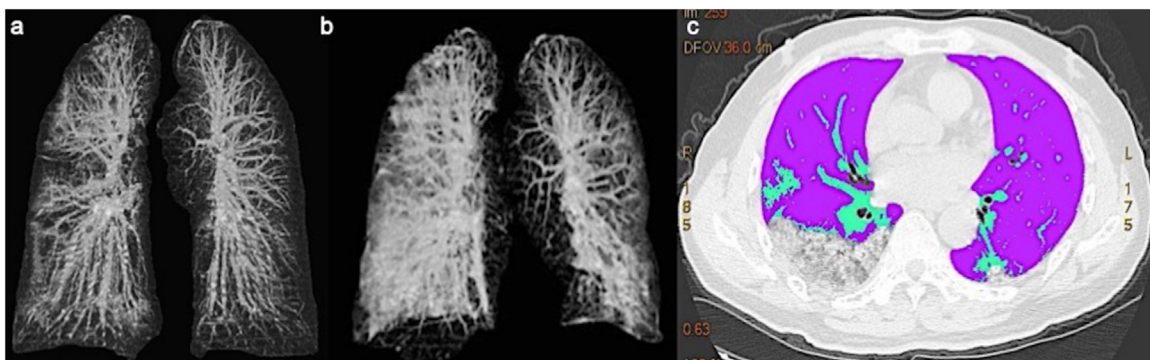

Figure 1. a,b,c. (a, b) Lung VCAR imaging displaying baseline CT and follow-up CT with progressive impairment of the lung parenchyma. (c) lung sparing analysis.

Figure 2. a,b. (a) Baseline chest CT images in a 66 years old man displaying multiple patchy ground glass opacities with reticular and interlobular septal thickening: crazy paving. The lesions are mostly distributed in the upper segment of right lower lobe and focal ground glass opacities in the superior segment of left inferior lobe. (b) Mediastinal lymphadenopathies the biggest with short axis of 12 mm.
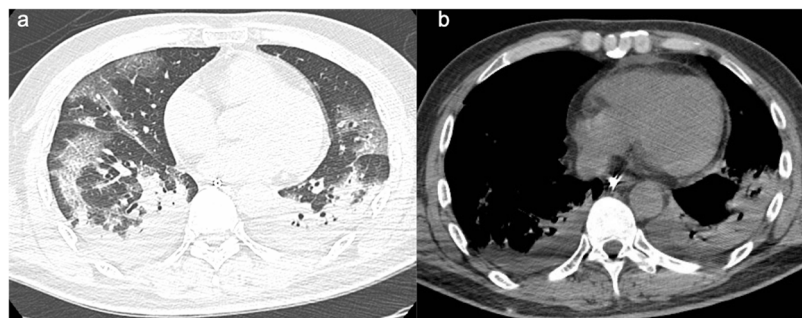

Figure 3. a,b. (a) Follow-up CT in a 66 years old man after 5 days, shows severe progression of pneumonia with increased of extension of ground glass opacities and consolidation. (b) Appearance of bilateral pleural effusion.

slight unilateral pleural effusion and mediastinal lymphadenopathies the biggest with a short axis of 12 mm (Figure 2b).

During the first follow-up CT scan on day 3, bilateral pleural effusion and pericardial effusion was noted (Figure 3b).

Lymph nodes with a ≥10 mm longitudinal size in the short-axis dimension were present in 2R, 4R, and 4L levels.

Sub-segmentary vessels increased in diameter in the first CT scan. There was a 5% and 10% increase in size after the third and sixth day of their follow-up.

In the female patient, a chest X-Ray was performed 2 days after symptom onset with evidence of interstitial lung alterations. On day 3, chest CT scan showed ground- glass and crazy paving in the anterior and posterior of the right upper lobe, in the middle segment of the middle lobe, in the superior and posterior-basal, as well as lateral basal segments of the right lower lobe. On the left side, the lesions involved the upper lobe and superior lobe, as well as the lateral-basal and posterior-basal segments of the lower lobe (Figures 4a, 5 a).

Non-pleural effusion appeared in the first and second CT examination and a bilateral pleural effusion appeared in the third CT examination. No pericardial involvement was reported (Figure 5b).

Nodes with a ≥10 mm longitudinal size in the short-axis dimension were present in the 1R, 6R, and 10R levels (Figure 4b).

Sub-segmentary vessels were increased in diameter size in the first CT scan. There was a 14% and 5% increase after the third and sixth day of their follow-up (Figure 6 a, b).

Both patients presented an increased number of lung impairment during their follow-up. A relative sparing of the anterior segment of both lower lobes was noted. This may due to the different distributions of airflow in the supine position.

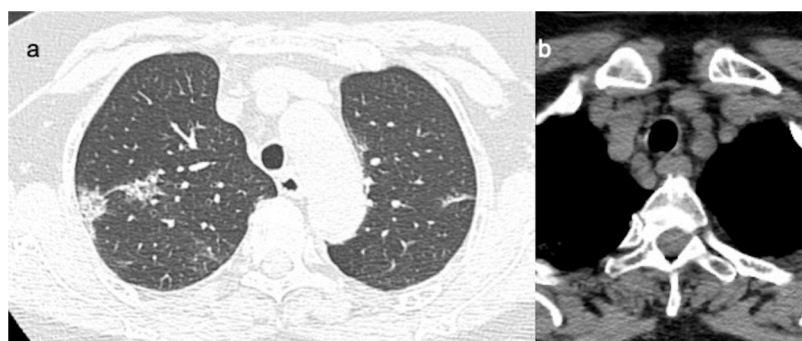**Figure 4. a,b.** (a) Baseline CT images in a 65 years old woman shows patchy ground-glass opacities in the posterior segment of upper right lobe, with pleural contact.(b) Mediastinal lymphadenopathy with short axis of 10 mm.
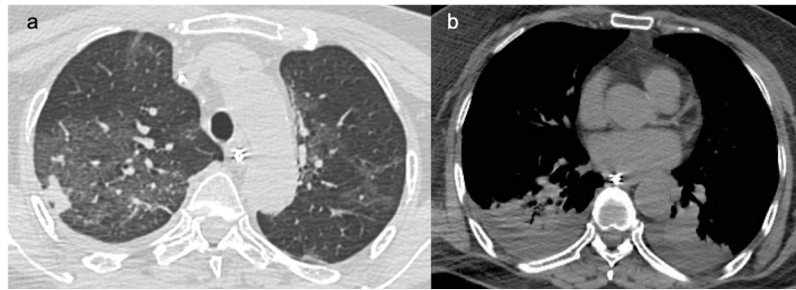
Figure 5. a,b. (a) Follow-up CT after 3 days in a 65 years old woman shows increase size and density of the lesions (b) with bilateral pleural effusion.
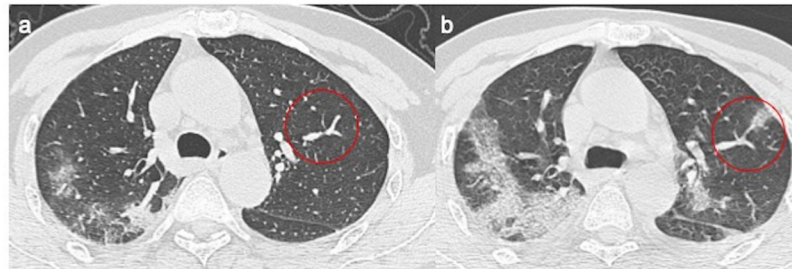

Figure 6. a,b. (a) Baseline chest CT shows tubular size increase of segmental vessel with normally ventilated adjacent lung parenchyma, (b) where after 3 days there is a ground-glass opacities.

There was an increase in number and size of lung lesion infiltrates with a relative increase in GGO, a reduction in interstitial-reticular involvement and an increase in consolidative areas in the posterior segments of the lower lobes.

Sequential data analysis in the baseline and follow-up CT scans of both patients are reported in Tables 1 and 2.

Discussion

Several recent studies (Chan et al., 2020; Chen et al., 2020; Chung et al., 2020; Kanne, 2020; Koo et al., 2018; Lei et al., 2020; Liu and Tan, 2020; Pan and Guan, 2020; Song et al., 2020; Wang et al., 2020) have described common chest imaging findings of lung pathology caused by SARS-COV2. The imaging findings recently reported in patients with COVID-19 appear similar to those reported with SARS-CoV (Ooi et al., 2004; Nestor et al., 2004; Nicolaou et al., 2003) and MERS-CoV (Das et al., 2015a; Das et al., 2015b) infection. Our patients showed some new and remarkable imaging findings seen in follow-up chest X-Rays and CT scans of these 2 cases who progressed to develop adult respiratory distress syndrome (ARDS). Lung patterns in both patients were characterized by hypertrophy of the pulmonary vessels, which are increased in size, particularly in areas with more pronounced interstitial impairment. This new radiological evidence suggests a different pattern of lung involvement compared to those observed in the other known severe coronavirus infections (SARS and MERS) (Ooi et al., 2004; Nicolaou et al., 2003) where pulmonary vessel vasoconstriction was possibly related to the presence of vasoactive substance within the lesions (Wenhui Li et al., 2003).

In these two cases, the increased diameter of the perilesional pulmonary vessels grew by extending the pulmonary alterations. During the follow-up examinations, a tubular and enlarged appearance of pulmonary vessels with a sudden caliber reduction was reported. They were mainly found in the dichotomic tracts, where the center of a new insurgent pulmonary lesion was seen (Figure 6a, b).

Table 1
Findings of Chest CT Patient 1 (age 67, gender M).

CT Findings	First CT	CT after 3 days	CT after 6 days
GGO and consolidation			
GGO	Y	Y	Y
Crazy paving	Y	Y	N
Consolidation	N	Y	Y
GGO + consolidation	N	Y	Y
Localization			
Right Upper Lobe			
Apical	Y	Y	Y
Posterior	Y	Y	Y
Anterior	Y	Y	Y
Middle Lobe			
Lateral	Y	Y	Y
Medial	N	Y	Y
Right Lower Lobe			
Superior	Y	Y	Y
Medial	N	Y	Y
Anterior	N	N	Y
Lateral	N	Y	Y
Posterior	Y	Y	Y
Left Upper Lobe			
Apical-Posterior	N	Y	Y
Anterior	N	Y	Y
Lingula	N	Y	Y
Left Lower Lobe			
Superior	Y	Y	Y
Medial	N	Y	Y
Anterior	N	N	Y
Lateral	N	Y	Y
Posterior	Y	Y	Y
>2 lobes affected	Y	Y	Y
Bilateral lung disease	Y	Y	Y
Pleural impairment	Y	Y	Y
Calcifications	N	N	N
Tracheal diameter (mm)	18 × 17	18 × 18	22 × 19
I–V increase (%)	–	5%	10%
Pleural effusion (mm)	N	Y	y
Lymphadenopathy	2R/4R/4L	2R/4R/4L	2R/4R/4L
CPA trunk diameter (mm)	25	25	25
Pericardial effusion	N	N	Y

GGO: Ground Glass Opacity; I–V: Intralesional Vessels.

Table 2
Findings of Chest CT patient 2 (age 65, gender F).

CT Findings	First CT	CT after 3 days	CT after 6 days
GGO and consolidation			
GGO	Y	Y	Y
Crazy paving	Y	Y	N
Consolidation	N	Y	Y
GGO + Consolidation	N	Y	Y
Localization			
Right Upper Lobe			
Apical	N	Y	Y
Posterior	Y	Y	Y
Anterior	Y	Y	Y
Middle Lobe			
Lateral	N	N	N
Medial	Y	Y	Y
Right Lower Lobe			
Superior	Y	Y	Y
Medial	Y	Y	Y
Anterior	N	N	N
Lateral	N	N	N
Posterior	Y	Y	Y
Left Upper Lobe			
Apical-Posterior	Y	Y	Y
Anterior	Y	Y	Y
Lingula	Y	Y	Y
Left Lower Lobe			
Superior	Y	Y	Y
Medial	N	Y	Y
Anterior	N	N	N
Lateral	Y	Y	Y
Posterior	Y	Y	Y
>2 lobes affected	Y	Y	Y
Bilateral lung disease	Y	Y	Y
Pleural impairment	Y	Y	Y
Calcifications (Nodules)	Y	Y	Y
Tracheal diameter (mm)	13 × 13	13 × 13	13 × 13
I–V vessels (%)	–	14	5
Pleural effusion	N	N	N
Lymphadenopathy	1/6/10R calcific	1/6/10R calcific	1/6/10 Rcalcific
CPA trunk diameter (mm)	28	30	30
Pericardial effusion	N	N	N

GGO: Ground Glass Opacity; I–V: Intralesional Vessels; CPA: Common Pulmonary Artery.

This sign is likely to be related to the hyperemia induced by the viral infection, and if consistent and validated by further observations, could be described as an early alert radiological sign to predict initial lung deterioration. Other findings of interest reported previously (Chung et al., 2020) were the presence in all scan examinations of mediastinal lymphadenopathy with short-axis oval nodes up to 1 cm and the presence of pleural effusion, first as unilateral and then subsequently bilateral; as it increased with the worsening of the symptoms.

Limitations of our findings

Our findings are specific only to two patients with a very short time interval between the follow-up CT scans, thus further studies are required to define the specific nature and importance of our findings. One of the patients presented radiological signs such as calcific nodules and lymphnodes of a possible previous infectious disease (i.e., tuberculosis). Finally, the unenhanced CT scan allows a limited evaluation of the pulmonary vascularity.

Conclusions

Although only two patients have been studied, these findings are consistent with the radiological pattern described in literature. Consistently with a previous report only (Chung et al., 2020), in both patients, pleural effusion and lymphadenopathy have been

reported. Finally, the pulmonary vessels enlargement in areas where new lung infiltrates develop in the follow-up CT scan, could describe an early predictor radiological sign of lung impairment. The full range of imaging findings in patients with SARS-COV2 infections will become clearer as more reports are published.

Conflict of interests

All authors have no conflict of interests.

Author declarations

GI and AZ are co-PIs of the European and Developing Countries Clinical Trials Partnership (EDCTP2) Programme, Horizon 2020, the European Union's Framework Programme for Research and Innovation, grants PANDORA-ID-NET. Sir Zumla is in receipt of a National Institutes of Health Research senior investigator award.

Permission and ethical approval

Consent was obtained from patient's daughter to have their images published.

Appendix A.

COVID 19 INMI Study Group

Maria Alessandra Abbonizio, Chiara Agrati, Fabrizio Albarello, Gioia Amadei, Alessandra Amendola, Mario Antonini, Raffaella Barbaro, Barbara Bartolini, Martina Benigni, Nazario Bevilacqua, Licia Bordi, Veronica Bordoni, Marta Branca, Paolo Campioni, Maria Rosaria Capobianchi, Cinzia Caporale, Ilaria Caravella, Fabrizio Carletti, Concetta Castilletti, Roberta Chiappini, Carmine Ciaralli, Francesca Colavita, Angela Corpolongo, Massimo Cristofaro, Salvatore Curiale, Alessandra D'Abramo, Cristina Dantimi, Alessia De Angelis, Giada De Angelis, Rachele Di Lorenzo, Federica Di Stefano, Federica Ferraro, Lorena Fiorentini, Andrea Frustaci, Paola Gallì, Gabriele Garotto, Maria Letizia Giancola, Filippo Giansante, Emanuela Giombini, Maria Cristina Greci, Giuseppe Ippolito, Eleonora Lalle, Simone Lanini, Daniele Lapa, Luciana Lepore, Andrea Lucia, Franco Lufrani, Manuela Macchione, Alessandra Marani, Luisa Marchioni, Andrea Mariano, Maria Cristina Marini, Micaela Maritti, Giulia Matusali, Silvia Meschi, Francesco Messina, Chiara Montaldo, Silvia Murachelli, Emanuele Nicastri, Roberto Noto, Claudia Palazzolo, Emanuele Pallini, Virgilio Passeri, Federico Pelliccioni, Antonella Petrecchia, Ada Petrone, Nicola Petrosillo, Elisa Pianura, Maria Pisciotta, Silvia Pittalis, Costanza Proietti, Vincenzo Puro, Gabriele Rinonapoli, Martina Rueca, Alessandra Sacchi, Francesco Sanasi, Carmen Santagata, Silvana Scarcia, Vincenzo Schininà, Paola Scognamiglio, Laura Scorzolini, Giulia Stazi, Francesco Vaia, Francesco Vairo, Maria Beatrice Valli.

References

Chan JF, Yuan S, Kok KH, To KK, Chu H, Yang J, et al. A familial cluster of pneumonia associated with the 2019 novel coronavirus indicating person-to-person transmission: a study of a family cluster. Lancet 2020;.

Chen N, Zhou M, Dong X, Qu J, Gong F, Han Y, et al. Epidemiological and clinical characteristics of 99 cases of 2019 novel coronavirus pneumonia in Wuhan, China: a descriptive study. Lancet 2020;.

Chung M, Bernheim A, Mei X, Zhang N, Huang M, Zeng X, et al. CT imaging features of 2019 novel coronavirus (SARS-COV2). Radiology 2020;200230.

Corman VM, Landt O, Kaiser M, Molenkamp R, Meijer A, Chu DK, et al. Detection of 2019 novel coronavirus (SARS-COV2) by real-time RT-PCR. Euro Surveill 2020;25(3).

Das KM, Lee EY, Al Jawder SE, Enani MA, Singh R, Skakni L, et al. Acute middle east respiratory syndrome coronavirus: temporal lung changes observed on the chest radiographs of 55 patients. AJR Am J Roentgenol 2015a;205(3):W267–74.

Das KM, Lee EY, Enani MA, AlJawder SE, Singh R, Bashir S, et al. CT correlation with outcomes in 15 patients with acute Middle East respiratory syndrome coronavirus. AJR Am J Roentgenol 2015b;204(4):736–42.

Huang C, Wang Y, Li X, Ren L, Zhao J, Hu Y, et al. Clinical features of patients infected with 2019 novel coronavirus in Wuhan, China. Lancet 2020;.

Kanne JP. Chest CT findings in 2019 novel coronavirus (SARS-COV2) infections from Wuhan, China: key points for the radiologist. Radiology 2020;200241.

Koo HJ, Lim S, Choe J, Choi SH, Sung H, Do KH. Radiographic and CT features of viral pneumonia. Radiographics 2018;38(3):719–39.

Lei J, Li J, Li X, Qi X. CT Imaging of the 2019 Novel Coronavirus (SARS-COV2) Pneumonia. Radiology 2020;200236.

Liu P, Tan XZ. 2019 Novel coronavirus (SARS-COV2) pneumonia. Radiology 2020;200257.

Nestor L, Müller GCO, Khong Pek Lan, Zhou Lin J, Tsang Kenneth WT, Nicolaou Savvas. High-resolution CT findings of severe acute respiratory syndrome at presentation and after admission. Am J Roentgenol 2004;182(1):39–44.

Nicolaou S, Al-Nakshabandi NA, Muller NL. SARS: imaging of severe acute respiratory syndrome. AJR Am J Roentgenol 2003;180(5):1247–9.

Ooi Gaik C, Khong PL, Müller Nestor L, Yiu Wai C, Zhou Lin J, Ho James CM, et al. Severe acute respiratory syndrome: temporal lung changes at thin-section CT in 30 Patients. Radiology 2004;230(3):836–44.

Organization WH. Novel Coronavirus(SARS-COV2) Situation Report – 19 2020. [Available from]:. 2020. https://www.who.int/docs/default-source/coronaviruse/situation-reports/20200208-sitrep-19-ncov.pdf?sfvrsn=6e091ce6_2.

Organization WH. Laboratory testing for 2019 novel coronavirus (SARS-COV2) in suspected human cases. Interim guidance. 2020.

Organization WH. World experts and funders set priorities for COVID-19 research. [Available from]:. 2020. https://www.who.int/news-room/detail/12-02-2020-world-experts-and-funders-set-priorities-for-covid-19-research.

Pan Y, Guan H. Imaging changes in patients with SARS-COV2. Eur Radiol 2020;.

Song F, Shi N, Shan F, Zhang Z, Shen J, Lu H, et al. Emerging coronavirus SARS-COV2 pneumonia. Radiology 2020;200274.

Wang C, Horby PW, Hayden FG, Gao GF. A novel coronavirus outbreak of global health concern. Lancet 2020;.

Wenhui Li MJM, Vasilieva Natalya, Sui Jianhua, Wong Swee Kee, Berne Michael A, Somasundaran Mohan, et al. Thomas C Greenough, Hyeryun Choe, Michael Farzan. Angiotensin-converting enzyme 2 is a functional receptor for the SARS coronavirus. Nature 2003;426(6965):450–4.